Multivariate Neuroanalysis with ANTsR: Application to Supervised Brain Segmentation

Nicholas J. Tustison[a,1], K. L. Shrinidhi[b], Jeffrey T. Duda[b], Philip A. Cook[b], Christopher Durst[a], James C. Gee[a], Murray C. Grossman[a], Max Wintermark[a], Brian B. Avants[b]

[a]*Department of Radiology and Medical Imaging, University of Virginia, Charlottesville, VA*
[b]*Penn Image Computing and Science Laboratory, University of Pennsylvania, Philadelphia, PA*

Abstract

Improvements in image acquisition and increasingly sophisticated statistical techniques for neuroanalysis have spurred the development of advanced computational frameworks for studying the brain—many of which have been made publicly available. One such popular toolkit is the open source Advanced Normalization Tools (ANTs) which contains a suite of well-vetted processing tools for core data transformation tasks such as image registration, image segmentation, inhomogeneity field correction and template building. However, despite the numerous solutions afforded by such tools, neuroscience (and data analysis in general) requires a statistical platform for making inferences with respect to given hypotheses once the requisite data transformations have been performed. In this paper, we describe the coupling of ANTs with the widely-used R language—an open source environment for statistical processing and data visualization—which we denote as ANTsR. One of the many benefits from such an integration is the accessibility to advanced statistical and machine learning techniques. To showcase the flexibility and power of ANTsR, we apply the combination of one such technique, Random Forests, and ANTs processing tools to the difficult problem of brain tumor segmentation. This includes evaluation on the public data set from the MICCAI 2012 BRATS challenge consisting of both real and simulated data. To facilitate reproducibility, all scripts and data used in this paper are publicly available for download.

Keywords: advanced normalization tools, BRATS, brain tumor segmentation, R project, random forests

1. Introduction

O

2. Materials and Methods

2.1. ANTsR: An ANTs/R Interface

2.1.1. Installation

The ANTsR package is publicly available on the github project hosting service.[2] Prior to installation of ANTsR, several external R packages need to be installed including: `Rcpp`, `signal`, `timeSeries`, `mFilter`, `doParallel`, `robust`, `magic`, `knitr`, `pixmap`, `rgl`, `misc3d` which is facilitated by the `install.packages()` mechanism. Additionally, in order to perform the supervised brain segmentation as described in later sections, one would need to also install `randomForest`, `snowfall`, `rlecuyer`, and `ggplot2`.

CMake[3] is an open source tool for the management and building of large-scale software projects. It is used to coordinate the downloading of external packages, such as the Insight Toolkit (ITK)[4] and ANTs. Detailed instructions for download and installation can be found on the ANTsR github website.

2.2. Supervised Brain Segmentation

2.2.1. Random Forests

Building on the developments of Ho [7] and Amit and Geman [1], Breiman introduced Random Forests for classification/regression [6] which performs relatively well against other machine learning strategies such as support vector machines and neural networks.

2.2.2. Multi-Modality Feature Image Preprocessing

Although several studies have pointed out the importance of intensity normalization and bias correction, our experience with the training data illustrated a degradation in performance when one or both steps (using [11] and [14], respectively) were performed due to the presence of the tumor/edema complex. Instead we simply windowed the image intensity for all images to be between the quantiles $[0.01, 0.99]$ and subsequently rescaled to $[0, 1]$. This strategy seemed to provide the best classification (probably due to the fact that the intensity corruption due to bias was relatively minimal in the data used). However, improved results might be obtained by a more sophisticated strategy in which an initial supervised segmentation is used to find the probabilistic estimates of the normal tissue locations (as done in this work) which could then be followed by using only the probabilistic maps of the normal tissues to construct a weight, or confidence, mask for estimating the inhomogeneity bias using N4 [14] followed by a repeated application of the supervised segmentation strategy described. Note that a similar iterative-based strategy until convergence is implemented in the ANTs

[1]Corresponding author: PO Box 801339, Charlottesville, VA 22908; T: 434-924-7730; email address: ntustison@virginia.edu.

[2]https://github.com/stnava/ANTsR

[3]http://www.cmake.org/

[4]http://www.itk.org/

script `antsAtroposN4.sh`.

2.2.3. Multi-Modality Feature Image Generation

Key to any supervised regression or classification protocol are the selected features for training and subsequent testing. Based on previous work and our own experience, we selected the following feature images to showcase the supervised segmentation strategy developed in this work.

- Per modality (FLAIR, T1, T1C, T2)
  - First-order neighborhood statistical images: mean, variance, skewness, and entropy. Neighborhood radius = 3.
  - GMM-based posteriors: CSF, gray matter, white matter, edema, and tumor
  - GMM connected component geometry features: volume, volume to surface area ratio, eccentricity, elongation
  - Template-based: symmetric template difference and contralateral difference. Gaussian smoothing (σ = 4mm).
- Misc.
  - Normalized Euclidean distance
  - Log Jacobian

For each modality, we create four first-order statistical feature images, five Gaussian mixture model (GMM)-based posterior probability feature images, four geometry features generated from the GMM posterior probability images based on connected components, and two difference images using symmetric template construction for a total of 4 modalities $\times$ (4 + 5 + 4 + 2) feature images per modality = 60 images. We employ two additional images consisting of the Euclidean distance image [9] created from the skull-stripped binary mask rescaled to the range [0, 1] and the log Jacobian image derived from the spatial normalization of the symmetric multivariate template and individual subject images. Given the intensity corrected images the corresponding multivariate template images, and a brain mask for each subject creation of all feature images is performed using the script `createFeatureImages.sh`.

Prior cluster centers for specific tissue types learned from training data [13] are used in the GMM to create multiple feature images. Given M tissue types (e.g. CSF, gray matter, white matter, edema, and tumor), a GMM formulates the probability distribution at each voxel, $\mathbf{x}$, as the sum of Gaussian components, $\mathcal{N}(\mathbf{x}|\mu, \sigma)$, i.e.

$$p\left(\mathbf{x}|\mu_m, \sigma_m, \lambda_m\right) = \sum_{i=1}^{M} \lambda_m \mathcal{N}(\mathbf{x}|\mu_m, \sigma_m) \tag{1}$$

where $\sum_{m=1}^{M} \lambda_m = 1$. One popular method for determining the parameters of the GMM is maximum likelihood estimation which can performed using the Atropos segmentation tool [3]. In contrast to previous generative modeling approaches for multi-modal tumor segmentation (e.g. [12, 15]), we do not use multivariate Gaussians to specify tissue probabilities but rather incorporate each univariate probability map into the feature vector of the training data. As pointed out in [10], multivariate modeling might obscure the distinct biological information provided by each modality. Instead, we let the random forest construction process determine the optimal combination of such multivariate information. Additionally, maximum posterior labeling from the GMM processing is used to determine the connected components for each label. Geometric features (assigned voxel-wise) include the physical volumes of each connected component including the volume to surface area ratio, the elongation, and eccentricity.

In order to better characterize deviations from normal multimodal brain shape and appearance, several features were derived using population-specific multivariate template construction. A recent neuroimaging reproducibility study by Landman et al. resulted in an open data cohort of 21 normal individuals, each imaged twice, comprising several modalities including arterial spin labeling, fluid attenuated inversion recovery (FLAIR), diffusion tensor imaging, functional imaging, T1, and T2 [8].

Given K image modality types for N subjects, $\mathbf{I} = \{I_1, I_2, \ldots, I_K\}$, multivariate template construction iterates between optimizing the set of diffeomorphic transforms between the subjects and the template, $\left\{\left(\phi_1, \phi_1^{-1}\right), \ldots, \left(\phi_N, \phi_N^{-1}\right)\right\}$ and constructing the optimal multivariate template appearance $\mathbf{J} = \{J_1, J_2, \ldots, J_K\}$ to minimize the following cost function:

$$\sum_{n=1}^{N} \left[D\left(\psi(\mathbf{x}), \phi_1^n(\mathbf{x}, 1)\right) + \sum_{k=1}^{K} \lambda_k \Pi_k \left(I_k^n\left(\phi_n(\mathbf{x}, 0.5)\right), J_k\left(\phi_n^{-1}(\mathbf{x}, 0.5)\right)\right) \right] \tag{2}$$

where D is the diffeomorphic shape distance,

$$D\left(\phi(\mathbf{x}, 0), \phi(\mathbf{x}, 1)\right) = \int_0^1 \|v(\mathbf{x}, t)\|_L dt \tag{3}$$

dependent on the choice of linear operator, L, and v is the velocity field

$$v\left(\phi(\mathbf{x}, t)\right) = \frac{d\phi(\mathbf{x}, t)}{dt}, \quad \phi(\mathbf{x}, 0) = \mathbf{x}. \tag{4}$$

Each pairwise registration employing the similarity metric Π_k can be assigned a relative weighting, λ_k, to weight a particular modality's influence in the construction process. Further theoretical details can be found in [2, 4]. In terms of implementation, this algorithm is encapsulated in the script `antsMultivariateTemplateConstruction.sh`, available in the ANTs repository, which permits parallel processing on an individual workstation or on a large computational cluster.

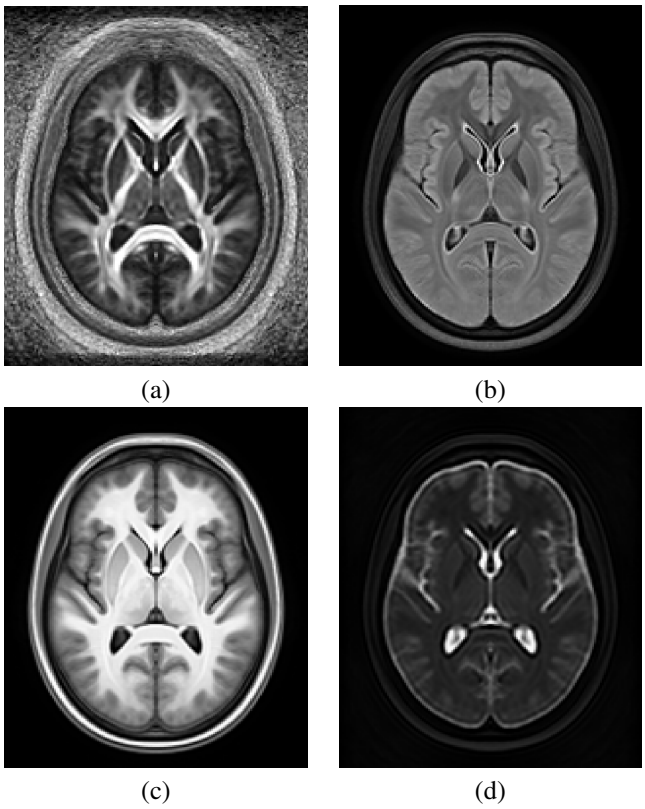

Figure 1: Multivariate symmetric template created from the Kirby 21 data described in [8]. Shown are the (a) fractional anisotropy (FA), (b) FLAIR, (c) MPRAGE, and (d) T2 template components.

2.2.4. Brain Tumor Segmentation Challenge Data

The Brain tumor segmentation Associated with the 2012 International Conference on Medical Image Computing and Computer Assisted Intervention (MICCAI),[5] the

2.2.5. MS lesion segmentation challenge Challenge Data

3. Results

4. Discussion and Conclusions

Acknowledgments

References

[1] Amit, Y., Geman, D., 1997. Shape quantization and recognition with randomized trees. Neural Computation 9, 1545–1588.

[2] Avants, B., Duda, J. T., Kim, J., Zhang, H., Pluta, J., Gee, J. C., Whyte, J., Nov 2008. Multivariate analysis of structural and diffusion imaging in traumatic brain injury. Acad Radiol 15 (11), 1360–75.

[3] Avants, B. B., Tustison, N. J., Wu, J., Cook, P. A., Gee, J. C., Dec 2011. An open source multivariate framework for n-tissue segmentation with evaluation on public data. Neuroinformatics 9 (4), 381–400.

[4] Avants, B. B., Yushkevich, P., Pluta, J., Minkoff, D., Korczykowski, M., Detre, J., Gee, J. C., Feb 2010. The optimal template effect in hippocampus studies of diseased populations. Neuroimage 49 (3), 2457–66.

[5] Bauer, S., Fejes, T., Slotboom, J., Wiest, R., Nolte, L.-P., Reyes, M., October 2012. Segmentation of brain tumor images based on integrated hierarchical classification and regularization. In: Proceedings of MICCAI-BRATS 2012. pp. 10–13.

[6] Breiman, L., 1996. Random forests. Machine Learning 24 (2), 123–140.

[7] Ho, T. K., 1995. Random decision forests. In: Document Analysis and Recognition, 1995., Proceedings of the Third International Conference on. Vol. 1. pp. 278–282 vol.1.

[8] Landman, B. A., Huang, A. J., Gifford, A., Vikram, D. S., Lim, I. A. L., Farrell, J. A. D., Bogovic, J. A., Hua, J., Chen, M., Jarso, S., Smith, S. A., Joel, S., Mori, S., Pekar, J. J., Barker, P. B., Prince, J. L., van Zijl, P. C. M., Feb 2011. Multi-parametric neuroimaging reproducibility: a 3-t resource study. Neuroimage 54 (4), 2854–66.

[9] Maurer, C. R., Rensheng, Q., Raghavan, V., 2003. A linear time algorithm for computing exact euclidean distance transforms of binary images in arbitrary dimensions. Pattern Analysis and Machine Intelligence, IEEE Transactions on 25 (2), 265–270.

[10] Menze, B. H., Van Leemput, K., Lashkari, D., Weber, M.-A., Ayache, N., Golland, P., 2010. A generative model for brain tumor segmentation in multi-modal images. Med Image Comput Comput Assist Interv 13 (Pt 2), 151–9.

[11] Nyúl, L. G., Udupa, J. K., Zhang, X., Feb 2000. New variants of a method of mri scale standardization. IEEE Trans Med Imaging 19 (2), 143–50.

[12] Prastawa, M., Bullitt, E., Moon, N., Van Leemput, K., Gerig, G., Dec 2003. Automatic brain tumor segmentation by subject specific modification of atlas priors. Acad Radiol 10 (12), 1341–8.

[13] Reynolds, D. A., 2009. Gaussian mixture modeling. In: Li, S. Z., Jain, A. K. (Eds.), Encyclopedia of Biometrics. Springer US, pp. 659–663.

[14] Tustison, N. J., Avants, B. B., Cook, P. A., Zheng, Y., Egan, A., Yushkevich, P. A., Gee, J. C., Jun 2010. N4itk: improved n3 bias correction. IEEE Trans Med Imaging 29 (6), 1310–20.

[15] Zikic, D., Glocker, B., Konukoglu, E., Shotton, J., Criminisi, A., Ye, D. H., Demiralp, C., Thomas, O. M., Das, T., Jena, R., Price, S. J., October 2012. Context-sensitive classification forests for segmentation of brain tumor tissues. In: Proceedings of MICCAI-BRATS 2012. pp. 1–9.

[5] http://www.miccai2012.org

Table 1: Dice scores from the MICCAI 2012 BRATs Study

Method	High-grade (real) Edema	High-grade (real) Tumor	Low-grade (real) Edema	Low-grade (real) Tumor	High-grade (simulated) Edema	High-grade (simulated) Tumor	Low-grade (simulated) Edema	Low-grade (simulated) Tumor
[15]	0.70 ± 0.09	0.71 ± 0.24	0.44 ± 0.18	0.62 ± 0.27	0.65 ± 0.27	0.90 ± 0.05	0.55 ± 0.23	0.71 ± 0.20
[5]	0.61 ± 0.15	0.62 ± 0.27	0.35 ± 0.18	0.49 ± 0.26	0.68 ± 0.26	0.90 ± 0.06	0.57 ± 0.24	0.74 ± 0.10
ANTsR	0.64 ± 0.18	0.65 ± 0.30	0.48 ± 0.16	0.69 ± 0.21	0.75 ± 0.25	0.94 ± 0.04	0.65 ± 0.25	0.83 ± 0.09